Enhanced electrochemical performance of acicular MnO$_2$ by adding conductive additive

XINGHUA LIANG[a*], XIAOMING HUA[a], YUSI LIU[a], SHUAIBO ZENG[a], HAIYAN CHEN[b]
aGuangxi Key Laboratory of Automobile Components and Vehicle Technology, Guangxi University of Science and Technology, Liuzhou 545006, Guangxi, China
bSchool of Materials and Energy, Guangdong University of Technology, Guangzhou510000, Guangdong, China

We have demonstrated a type of acicular manganese dioxide(MnO$_2$) via a facile chemical method. By adding different proportions of acetylene black (AB) or Multi-walled carbon nanotubes(MWCNTs) in MnO$_2$ as conductive additives, the capacitance of the electrodes with AB and MWCNTs has substantially increased about 30% compared with AB only at 0.25A/g and in the 0.5M Na$_2$SO$_4$ electrolyte. Moreover, the electrode with 15% MWCNTs shows the worst cyclic performance among those three electrode materials, which attribute to the rejection of the diffusion of ions in the electrolyte from the intensive conductive network of MWCNTs. However , the electrode with 5% MWCNTs and 10% AB has a great cycling performance at 78.3% capacitance retention over 1000 cycles. The morphology and structure of the MnO$_2$/AB/MWCNTs are systematically characterized by scanning electron microscope(SEM) and X-ray diffraction(XRD).

1. Introduction

Energy storage systems are playing significant roles in storing energy generated from sun and wind, or other renewable energy sources [1]. Supercapacitors, also called electrochemical capacitors or ultracapacitors, have attracted tremendous attention due to the fast charge/discharge characteristics, high power density and long cycle life [2].Generally, supercapacitors can be divided into pseudo-capacitors and electrochemical double-layer capacitors (EDLCs) in terms of the energy storage mechanism. They have been widely used in various applications.

Manganese oxide materials have attracted great attention due to their wide applications, such as in electrochemical supercapacitors [3], lithium-ion batteries [4], biosensors [5], molecular adsorption [6], and catalysis [7]. Such aspect of MnO$_2$ can also be exploited as one of the most promising candidates for electrochemical capacitors (ECs) electrodes materials with the consideration of its environmental benign nature, low cost, natural abundance and favorable pseudocapacitive characteristics. However, MnO$_2$ electrodes often suffer from poor electronic and ionic conductivities, resulting in their limited performance in power density and cycling [8]. Nanotubes have been constructed with length to diameter ratio of up to 132000000:1 [9], significantly larger than for any other material. These cylindrical carbon molecules have unusual properties used in many fields of materials science and technology. In this paper, we add MWCNTs into electrodes with AB as conductive additive and 15% in total for its enhanced electrical conductivity.

2. Experimental

6.32g KMnO$_4$ dissolved in 200ml DI water was added into 200ml DI water with MnCl$_2$·4H$_2$O dissolved in, then treated it in water baths at 60℃ while stirring for 12 hour. The product acicular MnO$_2$ obtained was washed with DI water for several times and died at 60℃ under vacuum. The electrode is consisted of 75% of MnO$_2$, 15% of conductive additive, and 10% of Polytetrafluoroethylene (PTFE). Then it was prepared as follows. Different conductive additive were divided into three groups: A(AB), B (m$_{AB}$:m$_{MWCNTs}$=2:1) and C(all MWCNTs). The mixture was stirring in DI water for 4 hours and ultrasounded for 15 minutes. The mixture containing 279.4mg as-prepared electroactive materials (A, B or C) and 5 drops of binder solution (60wt.% PTFE solution) was painted onto a nickel foam and then dried at 60℃. Then pressed it at 80mpa. The masses of active materials were determined by weighting the nickel foam before and after painting/drying.

CHI660d electrochemical workstation (Shanghai, China) was used to test the electrochemical performance of the electrodes. Electrochemical measurement was performed at room temperature in a three-electrode electro-chemical system: the testing electrode as working

electrode, a graphite electrode as the counter electrode, and a saturated calomel electrode (SCE) as the reference electrode. 0.5M Na_2SO_4 solution was used as electrolyte. Cyclic voltammetry (CV) measurement was performed between -0.2 and 0.8V with a variety of scan rates as 5,20,50,80,100mV/s, Galvanostatic charge-discharge (DCG) measurement was performed at different constant current densities as 0.25-1A/g, and electrochemical impedance spectroscopy(EIS) was carried out in the frequency range from 100 kHz to10 Hz.

The crystal structure and chemical composition were analyzed using X-ray diffraction (XRD) (DX2700, Liaoning, China) with CuKα radiation from 10° to 90°and respectively. The surface morphologies of the prepared electrodes were examined using scanning electron microscope (SEM) (S-3400N-II, Japan).

3. Results and discussion

3.1. Structure and morphology

The XRD patterns in Fig.1 shows the evidence of MnO_2, the diffraction peaks at 2θ values of ca. 12.784°, 18.107°, 28.841°, 37.522°, 41.968°, 49.864°, 60.274° are indexed to the reflections of α-MnO_2(Joint Committee on Powder Diffraction Standards (JCPDS) card No.

44-0141). Here found that the degree of crystallinity of MnO_2 is not perfect, that is ascribed to the material could not bear high temperature: it makes MnO_2 in collusion with O_2 from the air which redox reaction would happen in a temperature above 150℃. As the XRD reveals, the electrode material is proved to be a kind of α-amorphous MnO_2. In addition, the crystallinity and crystal structure have great influence on the performance of the MnO_2. Low degree of crystallinity is in favour of pore structure and high degree of crystallinity is good for conductivity. The sample we've got is moderate.
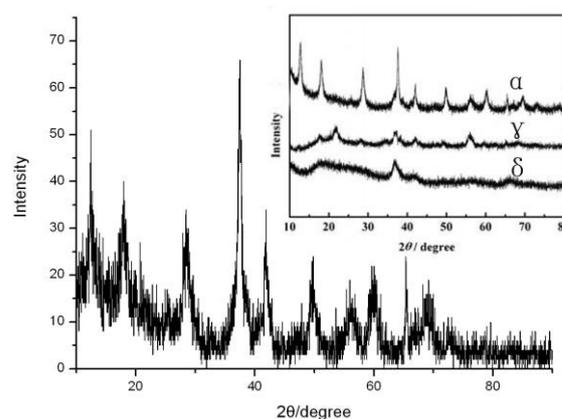

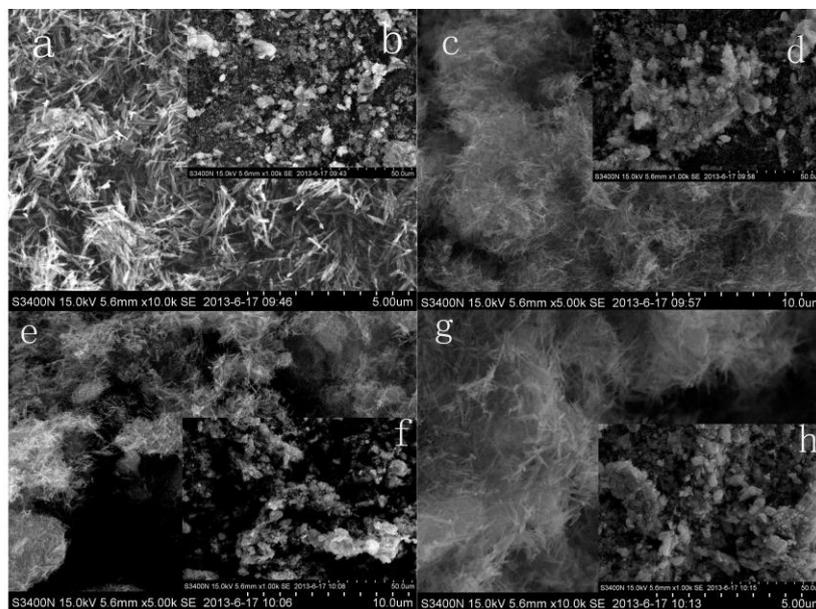*Fig.1. XRD patterns of α-MnO₂ and 3 types of MnO₂.*

Fig. 2. SEM images of the electrodes of MnO₂(a, b), A(c, c1, d), B(e, f) and C(g, h).

Fig. 2. reveals the morphology and structure of electrodes. Fig. 2(a) illustrates that MnO_2 nano-needles have a diameter about 40nm and length at about 1μm. The morphology of MnO_2 is dispersed uniformly. The neat acicular MnO_2 illustrates approximately several secondary particles of a few micrometers in diameter,

which is consisted of hundreds of primary particles described above (Fig. 2(a, b)), the diameter is ranging from 2 to 20μm (Fig. 2(b)). A few acicular MnO_2 primary particles have not agglomerated to form globular shape and disperse in small size. Image of the electrode of A (Fig.2(c)) shows the mixture particles of AB and MnO_2

whose sizes ranging from 10 to 25 μm (Fig. 2(c, d)). Acicular MnO_2 is coating and implanting to the particles of AB inside. The size of particles from A is a little larger compared to the particles from pure MnO_2(2 to 20μm(MnO_2), 10 to 25μm(A)). Electrode of C have less spherical structure which tend to be grow in mass and in line as well (Fig. 2(e, f)). The different shape and morphology between A and B may attribute to the content of spherical structure (AB) decreased while the content of MWCNTs in streaks increased with a scale of nano sizes. The particles are easy to grow together to have a size in diameter from 5 to 20μm when the content of conductive additive is MWCNTs only (Fig. 2(g, h)). It should be noted that the addition of AB and MWCNTs can form different morphologies and structures which reveals different electrical conductivity in the electrochemical properties follows.

3.2. Electrochemical properties

For comparative purpose, we should evaluate the electro-chemical performance of sample A, B and C. The CV measurements of A/B/C are performed in a potential range between -0.2 to 0.8V in 0.5M Na_2SO_4 neutral electrolyte with different scan rates (5, 20, 50 and 100mV/s, respectively). From the CV response currents in Fig. 3 (A), the electrode of A is reversibly well and oxidized. The redox features of the anodic and cathodic peaks at all the scan rates suggest the pseudocapacitive process for the material in the electrolyte assign. The morphology of particles in Fig. 3 (B) is as the same as that in Fig. 3(A). However, the CV curves of 50mv/s and 100mv/s is abnormally almost the same (Fig. 3 (C)), which shows a poor performance under heavy current.
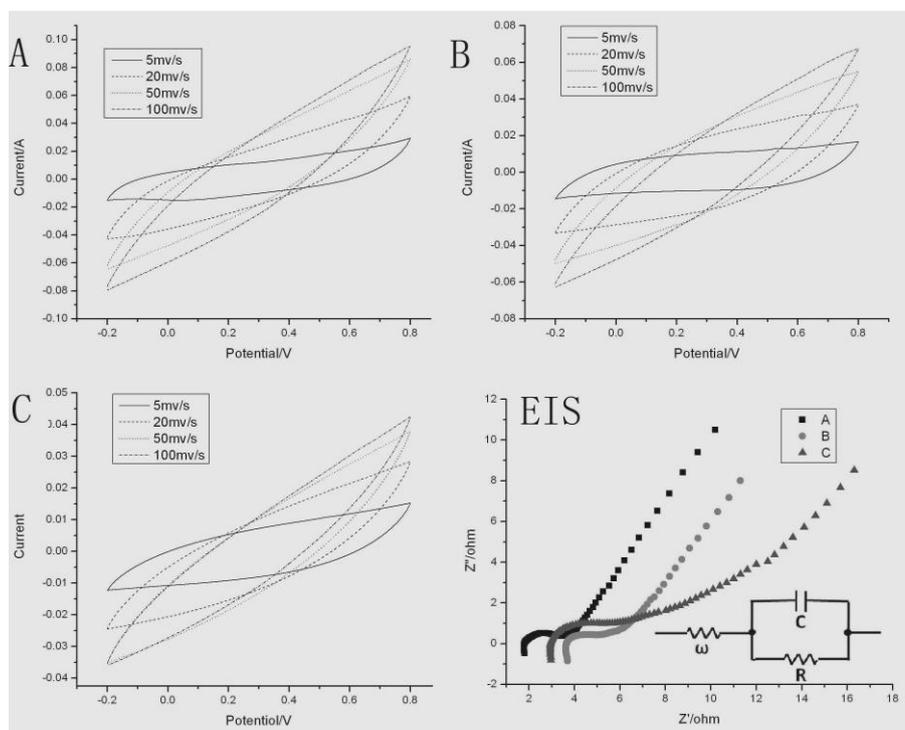

Fig.3. CV curves of A,B and C in 0.5M Na_2SO_4. (EIS) EIS spectra for electrodes of A, B and C.

The typical GCD curves of A/B/C at different current densities (0.25, 0.5, 1A/g) are demonstrated in Fig.4 (A, B, C). The charge/discharge cycle for the electrodes was performed in 0.5M Na_2SO_4 neutral electrolyte at current density of 0.25, 0.5 and 1A/g between -0.2 and 0.8V. The discharge profiles of the asymmetric and symmetric capacitor show a typical capacitive behavior with a linear slope. All curves are shown as triangles. Curves of C show a poor chemical performance because of the charge time is much longer than the discharge time and the Symmetry is poor. These results accord with Fig. 4 (A, B, C) which calculated by following equations from the constant current charge/discharge cycle:

$$Cm=C/M=It/\Delta vm \qquad (1)$$

Where I, t, Δv and m, respectively, indicate the constant discharge current, the discharge time, the efficient electrochemical window and the mass loading of electrode material.

GCD measurements at different current densities are applied to quantify the specific capacity (SC) and to evaluate the electrochemical properties. Fig. 4 (A, B, C) shows the typical GCD curves of the materials between −0.2 and 0.8V at different current densities as indicated. The SC of the materials are obtained and listed in Table 1, respectively.

Table 1. The SC of the A, B and C electrolytes.

Electrodes of different conductive additive	SC(F/g) (0.25A/g)	SC(F/g) (0.5A/g)	SC(F/g) (1A/g)
A	64.75	50.35	34.60
B	83.50	50.95	28.20
C	40.53	27.90	14.00

From the data demonstrated in Table1, B have a better SC(83.5 F/g) as to A(64.75F/g) or C(40.35F/g) at the current density of 0.25A/g, while sharing the same SC(50.53 and 50.95F/g) at the current density of 0.5A/g. A(34.6F/g) has a better performance of SC than B(28.2F/g) at the current density of 1A/g. In short, SC values of A   is beyond B and C generally.

The electrochemical impedance of the electrode A, B and C   were examined over the frequency range of 10kHz–10Hz at a dc bias of 0V with a sinusoidal signal of 2mV as shown in Fig. 4(EIS). A semicircular loop in high frequency followed by a nearly vertical straight line in the low frequency is observed. The EIS spectra and the impedance data analyzed on the basis of the equivalent circuit are shown in Fig. 4(EIS). R is the resistance of the electrolytes. Calculated by following equations:

$$(Z'')^2+(Z'-R/2)^2=(R/2)^2 \qquad (2)$$

Where Z is the total impedance, Z' and R is the internal resistance, and Z'' is the capacitive reactance of the system. R(A) is 1.316Ω, R(B) is 1.098Ω and R(C) is 2.277Ω as the parameters fitted by Zview software. It concludes that R(C) >R(A)> R(B).

Long cycling life is another considerable issue for supercapacitor electrodes (Fig. 4(D)). The cycling life tests over GCD cycles for the electrodes of A, B and C were carried out which under the current density of 1A/g. Fig. 4(D) shows that two of the three electrodes   have a decrease in available specific capacity. Fig of material A gets terribly decrease after circulate 150 cycles and keeps stable in the 200 cycles later. A big fall appears in the rest cycles. Electrode B shows a decrease in the initial 200 cycles and in the rest 400 cycles, the stable capacity of the electrode suggests a good cycling life. A small decrease appears in the last 300 cycles. Electrode C has a cycle life for just 20 times then stop working. The reason for this phenomenon may due to the adding of the conductive additive of the electrode material. When the adding of MWCNTs is 5% only, MWCNTs companied with each other so that a net of MWCNTs has been built, and improve the conductivity of the material. When the amount of CNTs increased to 15%, the net become much thick which preventing the shuttle of the ions in the solution in reverses.
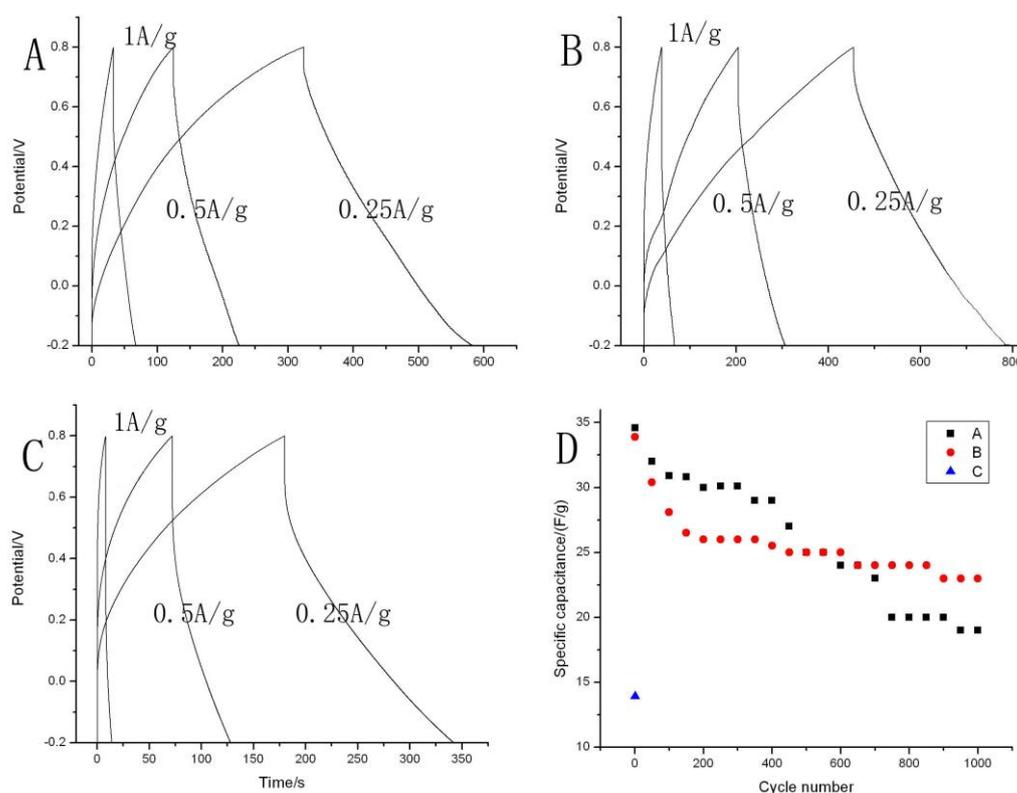

Fig. 4. (A), (B), (C)GCD curves for A, B and C at current density of 0.25, 0.5 and 1A/g. Variation of specific capacitance charging–discharging cycle number for A, B and C at 1A/g in 0.5M Na$_2$SO$_4$.

4.Conclusions

MWCNTs were used to improve the electrochemical performance of MnO_2 in supercapacitors. MWCNTs were intersected into the MnO_2 particles by physical method and built a 3D conductive network through the MnO_2 molecule. When 5% MWCNTs and 10% AB were compounded into the MnO_2 as conductive additives, the specific capacity of MnO_2/CNTs/AB composite electrodes delivered of 83.50F/g, 50.95F/g and 28.20F/g under different current density as 0.25A/g, 0.5A/g and 1A/g respectively. This group was the best of those three samples. Only when the conductive additive became MWCNTs, the net of MWCNTs could be stronger and denser. Though the conductive of electrode has been increased, the diffusion of the ions in the electrolyte was restrained. Much ions may be locked into the thick net of MWCNTs because of the   special interior structure, which made the material owned poor cyclic life and the worst specific capacity as 40.53 F/g, 27.90 F/g and 14.00 F/g under the same current density as B, even lower than the electrode material with pure AB.

References

[1] Qiang Lia, Jianhua Liu, Jianhua Zou, Anindarupa Chunder, Yiqing Chen, Lei Zhai, Journal of Power Sources., **196**, 565 (2011).
[2] Wenbo Zhang，Bin Mu，Aiqin Wang, J Mater Sci., 2013.
[3] Zhang, H., Cao, G., Wang, Z., Yang, Y., Shi, Z., Gu, Z., Nano Lett., **8,** 2664 (2008).
[4] Luo, J. Y., Zhang, J. J., Xia, Y. Y., Chem. Mater., **18,** 5618 (2006).
[5] Chen, J., Zhang, W. D., Ye, J. S., Electrochem. Commun., **10,**1268 (2008).
[6] Zhai, Y., Zhai, J., Zhou,M., Dong, S., Mater. Chem., **19**, 7030 (2009).
[7] Zhang, L., Liu, C., Zhuang,L., Li, W., Zhou, S., Zhang, J., Biosens. Bioelectron.,**24**, 2825 (2009).
[8]Guihua Yu, Liangbing Hu, Nian Liu, Huiliang Wang, Michael Vosgueritchian, Yuan Yang, Yi Cui, Zhenan Bao, J., Nano Lett., **11**, 4438 (2011).
[9] Wang X., Li Qunqing, Xie Jing, Jin Zhong, Wang Jinyong, Li Yan, Jiang Kaili, Fan Shoushan, Nano Letters, **9**(9), 3137 (2009).

Corresponding Author: captainhua@gmail.com